

Charge-Shift Bonding—A Class of Electron-Pair Bonds That Emerges from Valence Bond Theory and Is Supported by the Electron Localization Function Approach

Sason Shaik,^{*,[a]} David Danovich,^[a] Bernard Silvi,^{*,[b]} David L. Lauvergnat,^[c] and Philippe C. Hiberty^{*,[c]}

Dedicated to Yitzhak Apeloig on occasion of his 60th birthday

Abstract: This paper deals with a central paradigm of chemistry, the electron-pair bond. Valence bond (VB) theory and electron-localization function (ELF) calculations of 21 single bonds demonstrate that along the two classical bond families of covalent and ionic bonds, there exists a class of charge-shift bonds (CS bonds) in which the fluctuation of the electron pair density plays a dominant role. In VB theory, CS bonding manifests by way of a large covalent-ionic resonance energy, RE_{CS} , and in ELF by a depleted basin population with large variances (fluctuations). CS bonding is shown to be a fundamental mechanism that is

necessary to satisfy the equilibrium condition, namely the virial ratio of the kinetic and potential energy contributions to the bond energy. The paper defines the atomic propensity and territory for CS bonding: Atoms (fragments) that are prone to CS bonding are compact electronegative and/or lone-pair-rich species. As such, the territory of CS bonding transcends considerations of static charge distribution, and in-

volves: a) homopolar bonds of heteroatoms with zero static ionicity, b) heteropolar σ and π bonds of the electronegative and/or electron-pair-rich elements among themselves and to other atoms (e.g., the higher metalloids, Si, Ge, Sn, etc), c) all hypercoordinate molecules. Several experimental manifestations of charge-shift bonding are discussed, such as depleted bonding density, the rarity of ionic chemistry of silicon in condensed phases, and the high barriers of halogen-transfer reactions as compared to hydrogen-transfers.

Keywords: bond theory • charge-shift bonding • electron pairing • ELF (electron localization function) • valence bond

[a] Prof. S. Shaik, Dr. D. Danovich
Department of Organic Chemistry and the Lise-Minerva Center for Computational Chemistry
The Hebrew University, Jerusalem 91904 (Israel)
Fax: (+972) 658-4680
E-mail: sason@yfaat.ch.huji.ac.il

[b] Prof. B. Silvi
Laboratoire de Chimie Théorique, UMR CNRS 7616
Université de Paris-6, 4 Place Jussieu
75252 Paris Cédex (France)
Fax: (+33) 01-44-27-41-17
E-mail: silvi@lct.jussieu.fr

[c] Dr. D. L. Lauvergnat, Prof. P. C. Hiberty
Laboratoire de Chimie Physique, UMR CNRS 8000, Groupe de Chimie Théorique, Université de Paris-Sud, 91405 Orsay Cédex (France)
Fax: (+33) 1-69-41-61-75
E-mail: philippe.hiberty@lcp.u-psud.fr

Supporting information (ELF theory and comparisons of BOVB, VBCI, and benchmark CCSD(T) results) for this article is available on the WWW under <http://www.chemeurj.org/> or from the authors.

Introduction

There are probably only a handful of concepts that are as fundamental and central to chemistry as the concept of the electron-pair bond. This concept was formulated by Lewis in his 1916 paper,^[1] and eventually given a theoretical basis in 1927, when Heitler and London published their seminal work,^[2] which showed that the bond energy in H_2 can be viewed to arise from the resonance interaction between the two spin arrangement patterns, $H^\uparrow H^\downarrow$ and $H^\downarrow H^\uparrow$, required to generate a singlet electron pair. The quantum-mechanical articulation of Lewis's shared-pair model has culminated in the generalizing intellectual construct of Pauling,^[3] who described the electron pair bond $A-X$ as a superposition of covalent (Φ_{cov}) and ionic forms, $\Phi_{A^+X^-}$ and $\Phi_{A^-X^+}$ (Figure 1), and thereby enabled a unified description of bonding in any molecule, in terms of the method known since then as valence bond (VB) theory. Around the same time, Slater

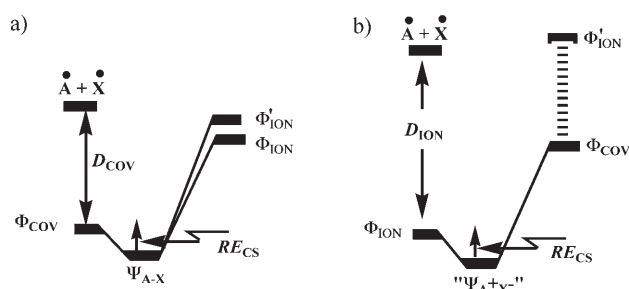


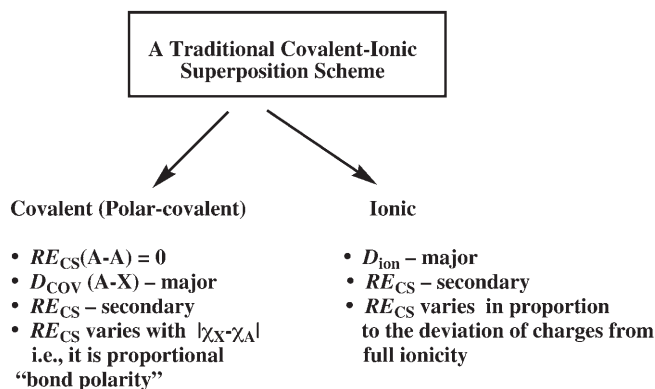
Figure 1. The classical Pauling's paradigm of covalent-ionic superposition in an A–X bond. a) A–X bond with predominant covalent character. b) A–X bond with predominant ionic character.

showed^[4] that a molecular orbital (MO) treatment followed by complete configuration interaction is equivalent to the VB-based covalent-ionic scheme of Pauling.

Figure 1 describes the key elements of Pauling's classical paradigm of covalent-ionic superposition. Three structures, one covalent, Φ_{COV} , and two ionic, $\Phi_{\text{A}^+\text{X}^-}$ and $\Phi_{\text{A}^-\text{X}^+}$, describe any A–X bond, which may either be homo- or heteronuclear. The covalent structure is stabilized by spin-pairing, owing to the resonance of the $\text{A}^\uparrow\text{X}^\downarrow$ and $\text{A}^\downarrow\text{X}^\uparrow$ spin arrangement forms. For a dominantly covalent bond, where Φ_{COV} is the lowest VB structure (part a), this stabilization energy is the covalent contribution, D_{COV} , to the total bonding energy. On the other hand, ionic structures are stabilized by electrostatic interactions, relative to the separated atoms by an amount D_{ION} . When an ionic form, for example, $\Phi_{\text{A}^+\text{X}^-}$, is the lowest among the VB structures (part b), the bond is ionic and the electrostatic stabilization energy is the ionic contribution to the bond energy.^[5,6] The covalent-ionic mixing results in a resonance energy contribution that augments, in principle, the bonding of either covalent or ionic bonds. In the past we referred to this quantity as the “charge-shift resonance energy”, RE_{CS} ,^[7] because the pair density inherent in the VB wave function shows that *covalent-ionic mixing is associated with fluctuation of the electron pair from the average electron population*. As we shall see later, the RE_{CS} quantity figures prominently in the bonding motif that is in the focus of this paper.

The Pauling scheme in Figure 1 has two major problems: First, the covalent structure is assumed to be *always bonded relative to the separated atoms*, since the covalent bond energy, D_{COV} , is estimated as the average bond energies of the two homopolar bonds A–A and X–X. Second, since this formula always overestimates D_{COV} it will always underestimate the role of RE_{CS} .^[8,9] As shown later, this assumption about D_{COV} is incorrect, and its implementation leads to a loss of essential features, which are in the focus of this work.

In practice, and as a result of the above problems, the Pauling scheme for covalent-ionic superposition has traditionally become associated with two bond-families, based on a criterion of static charge distribution; these are the covalent bond and ionic bond families in Scheme 1. In the first family, the major contribution to bonding comes from spin-pairing. In homonuclear bonds the RE_{CS} contribution was



Scheme 1. The traditional covalent and ionic bond families based on Pauling's covalent-ionic superposition scheme.

assumed, in Pauling's original scheme^[8a] and thereafter, to be very small and *was set to zero*. In polar-covalent bonds, the primary contribution to bonding is normally considered to be the D_{COV} quantity,^[8b] while the charge-shift resonance energy is of secondary importance, except for very polar bonds.^[9] Furthermore, the magnitude of RE_{CS} is considered to vary in proportion to the electronegativity difference of the fragments, A and X, much like the charge distribution in $\text{A}^{+\delta}\text{X}^{-\delta}$, that is, the “bond-polarity”.^[9]

In the second family, the major bonding contribution comes from the electrostatic energy in the dominant ionic structure, while the charge-shift resonance energy is a minor factor; its magnitude is supposed to vary in proportion to the deviation of the charge distribution from full ionicity. As such, in the traditional classification of both bonding types, it is assumed that one can deduce the magnitude of the covalent-ionic resonance energy *by simple inspecting of the static charge distribution of the molecule*.

Using MO theory, it is possible to transform the delocalized canonical MOs to a set of localized MOs (LMOs) that describe two-center bonds.^[10] The LMOs retrieve the covalent-ionic superposition scheme as follows: The electron-pair bond is the LMO itself, while the covalent-ionic superposition can be quantified from the charge polarization of the LMO, that is, from the coefficients of the hybrids that belong to the contributing fragments to the LMO; the relative sizes of these coefficients determine the bond polarity. Accordingly, MO theory leads to the same electron-pair bonding picture as the classical covalent-ionic paradigm of Pauling. In fact, both VB and MO descriptions support the Lewis formulation of electron pair bonding.

Thus, our bonding paradigm is now 89 years old, and yet even a cursory search in the literature suggests that this is perhaps not the whole story.^[5] Just consider the bonds of silicon to electronegative atoms. In terms of the static charge distribution, these bonds are virtually as ionic as for example, LiF or NaCl (e.g., $\text{H}_3\text{Si}^{+0.85}\text{F}^{-0.85}$ versus $\text{Li}^{+0.94}\text{F}^{-0.94}$, $\text{Na}^{+0.91}\text{Cl}^{-0.91}$, etc).^[11,12] But, while Li^+F^- and Na^+Cl^- behave as a genuine ionic bonds, the “ Si^+X^- ” bonds behave chemically as covalent bonds.^[13–15] The bonds look so similar, yet they are so very different in their chemical behavior.

Indeed, all Si–X bonds are more ionic than the corresponding C–X bonds,^[13] by virtue of static charge distribution, and nevertheless, these are the C–X bonds that exhibit “ionic” chemistry in condensed phases, whereas the ionic Si–X chemistry is extremely rare with a handful of exceptions.^[13–15] For example, trityl perchlorate is an ionic solid, $\text{Ph}_3\text{C}^+ \text{ClO}_4^-$, like NaCl,^[14b] while the silicon analogue, is a covalent solid, with a short Si–O bond.^[14c] It is apparent therefore, that the static charge distribution is not necessarily a reliable indicator of the nature of bonding. *There must be an additional property of the bond that is missing in the traditional covalent-ionic superposition scheme and that makes this difference between the various “ionic bonds”.*

These, and many similar puzzles, have prompted some of us in 1990 to reexamine the classical covalent-ionic paradigm using the tools of modern VB theory.^[7] Our first intriguing finding^[7a,b] concerned the F–F bond, which by any known measure would be defined as a covalent bond. First, it is a homonuclear bond, where ionicity should not matter. Second, the weight of its covalent structure is as large as that for the H–H bond.^[7a,b] Is the F–F bond really covalent as the H–H bond?

The counterintuitive answer in Figure 2b versus Figure 2a is a definite no. Figure 2 displays the dissociation energy curves of H_2 and F_2 for the covalent VB structure alone and for the “exact” ground state, which is a resonating combination of the covalent and ionic components. It is apparent that the bonding natures of the H–H and F–F bonds are very different. While in H_2 the covalent component alone displays a potential well which is already a good approximation of the exact curve (Figure 2a), the covalent component of F_2 is on the contrary purely repulsive (Figure 2b), and *the bonding is in fact sustained by the very large charge-shift resonance energy.*^[16] Thus, although F–F is formally a covalent bond, by virtue of its zero static charge distribution, this definition is not telling its true nature; the F–F bond is in fact a charge-shift bond (CS bond), because *the bonding exists as a result of the ionic-covalent fluctuation of the electron pair density.* This example shows that the assumption^[8a] underlying the classical Pauling scheme is incorrect; the covalent bonding by itself is not necessarily stabilizing even for homopolar bonds, and even in case where the covalent structure dominates the wave function, as in F–F. And furthermore, *homopolar bonds can have very large charge-shift resonance energies.*

In recent years, a variety of σ and π bonds, both homo- and heteronuclear, were shown to share this property, thereby forming a growing family of CS bonds.^[7] The emergence of the CS bond family and the eventual acceptance of the idea would revise the electron-pair bond concept in chemistry. One prerequisite for such a revision is the alternative and independent theoretical derivations of the CS bonding phenomenon, and most importantly, drawing links to experimental data.

An alternative way to look at bonding is through the electron density analyses of the molecule.^[11b,17–21] The peculiarity of F–F and a few other bonds has been noted since the late

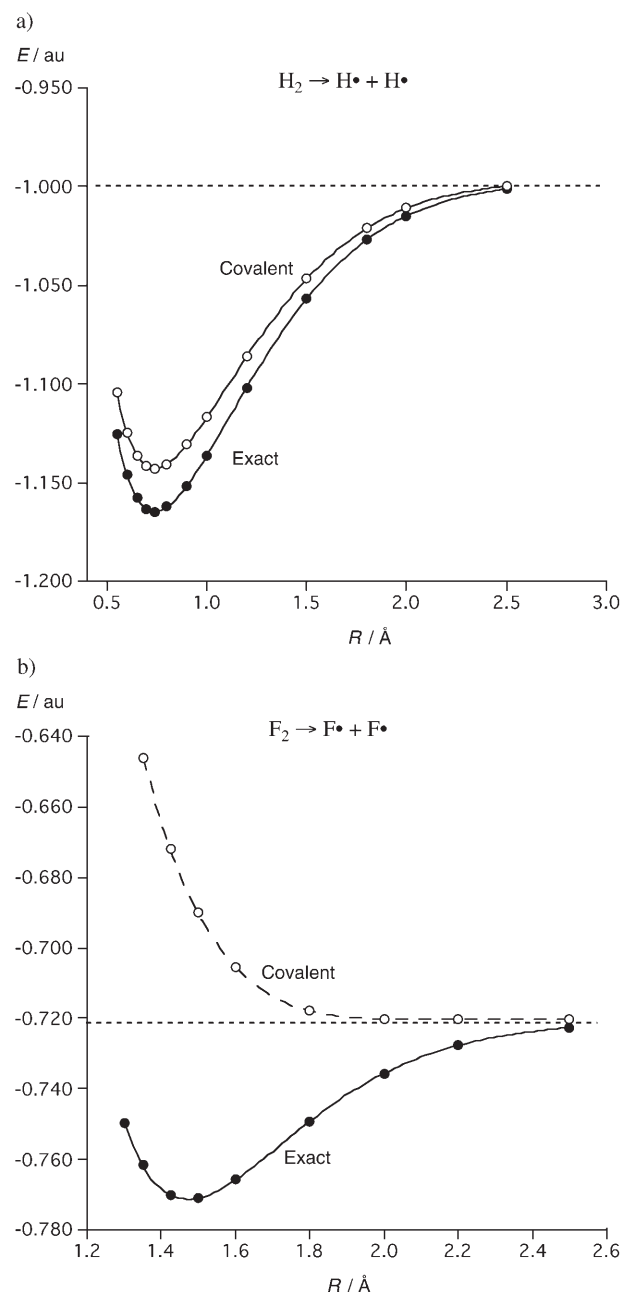


Figure 2. Dissociation energy curves for a) H_2 and b) F_2 . Dotted lines, open circles: the purely covalent VB structure. Bold lines, filled circles: the optimized covalent + ionic “exact” ground state.

1960s based on the electron-density perspective of bonding. For example, two different types of density analyses, the theory of atoms in molecules (AIM)^[11b,17] and the electron localization function (ELF) approach,^[19,20] demonstrate that the F–F molecule has very little electron density in the bonding region, which exhibits a *repulsive closed-shell like interaction*, as shown in Figure 3.^[17b,20,21e]

Furthermore, Rincon and Almeida^[21e] analyzed the density of VB-type wave functions and concluded that the dominant covalent character of F–F does not conform to “the shared-type interaction”. These electron density-based re-

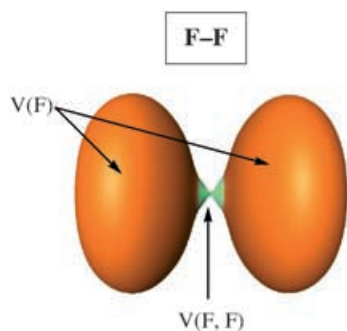


Figure 3. ELF localization domains of F_2 . Color code: orange: monosynaptic; green: disynaptic. Note the highly depleted and disjointed bonding region.

sults regarding the nature of the F–F bond parallel the energy-based VB picture (Figure 2), in which the covalent structure of the bond is by itself repulsive, while *the bonding is sustained by the covalent-ionic fluctuation of the bond*. Thus, anyway one looks at the bond in F–F, this bond is fundamentally different from the paradigmatic covalent bond,^[16] and as such an investigation is called for of the nature and the territory of this bond-type, so-called CS bond. To explore the territory of CS bonding, we undertook a dual and systematic study of the nature of a variety of two-electron bonds, using two independent theoretical methods, modern VB theory and density functional theory (DFT) followed by an ELF analysis, with the goal of providing complementary insight into this bond-type. Thus, while the VB approach will provide the energy perspective, the ELF approach will outline the complementary electron density perspective. As shall be demonstrated, both VB and ELF theories show that *CS bonding is a ubiquitous and distinct class of bonding that transcends formal “ionicity”*; it exists alongside the traditional covalent and ionic bond families and provides the missing bonding property necessary to understand many of the aforementioned puzzles.

Theoretical Methods

Modern VB methods: The principles of modern VB theory have been recently reviewed.^[22] The VB methods that incorporate dynamic correlation and are used in the present study were described elsewhere.^[23,24] These are the breathing orbital VB (BOVB) method,^[23] and the VB configuration interaction (VBCI) method,^[24] which are briefly outlined. In both methods, the bond is described by the wave function given in Equation (1), where the c denotes structural coefficients and Φ denotes covalent and ionic VB structures that distribute the electron pair between the orbitals of the two bonded fragments; these orbitals are called the active orbitals.

$$\Psi_{A-X} = c_{\text{COV}}\Phi_{\text{COV}} + c_{A^+X^-}\Phi_{A^+X^-} + c_{A^-X^+}\Phi_{A^-X^+} \quad (1)$$

The remaining electrons (inactive-shell), of each VB structure, are arranged in doubly occupied orbitals.

In the BOVB method, the structural coefficients and orbitals of the VB structures are optimized, and a dynamic correlation is introduced by allowing the orbitals to assume sizes and shapes that are different for the different structures. In the VBCI method,^[24] initially, the coefficients and orbitals are optimized, the latter as a common set for the three fundamental VB structures, as in the valence-bond-self consistent field (VBSCF) method.^[25] Subsequently, dynamic correlation is introduced by singles and doubles configuration interaction (CI) from the optimized orbitals of the fundamental structures into virtual orbitals. The virtual orbitals are constrained to be localized on the same bonds as the occupied orbitals.^[24] In this manner, the excited VB structures keep the same spin-pairing and charge characters as the fundamental structures, and it is therefore possible to contract each fundamental structure and its excited ones into a single structure, covalent or ionic as in Equation (1). The final VBCI wave function has the same dimension as the one expressed by Equation (1).

The charge-shift resonance energy, RE_{CS} , is defined in Equation (2) as the difference between the lowest energy structure Φ_i and the full wave function of Equation (1) (see also Figure 1).

$$RE_{\text{CS}} = E(\Phi_i) - E(\Psi_{A-X}); \Psi_i = \Phi_{\text{COV}} \text{ or } \Phi_{A^+X^-} \quad (2)$$

Here both $E(\Phi_i)$ and $E(\Psi_{A-X})$ are determined *variational* within their respective spaces of VB structures, and as such, the RE_{CS} quantity is quasi-variational.

The weights of the VB structures are determined by using the Coulson–Chirgwin^[26] formula, [Eq. (3)], which is the equivalent of a Mulliken population analysis in VB theory.

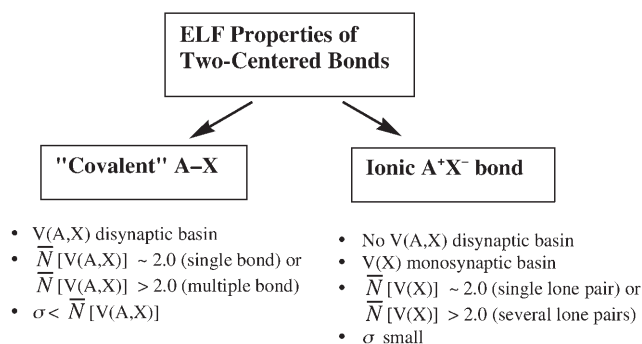
$$\omega_i = c_i^2 + \sum_{j \neq i} c_i c_j \langle \Phi_i | \Phi_j \rangle; \quad (\Phi_i, \Phi_j : \text{covalent and ionic structures, [Eq. (1)]}) \quad (3)$$

The trends in the weights arising from Equation (3) do not change if instead of the Coulson–Chirgwin formula one uses Löwdin weights, which are derived from the squares of the coefficients after renormalization.^[27] Qualitatively, the VB structure with the lowest energy in the wave function will possess the largest coefficient and hence, also the largest weight according to Equation (3) or to a Löwdin analysis. Thus, the weights of Equation (3) are valid whether a given structure is bonded or repulsive. For example, in the case of the F–F bond (Figure 2b above), the weight of the covalent structure is going to be the dominant weight since Φ_{COV} is the lowest VB structure. The same would apply to H–H, where now the Φ_{COV} structure is bonded (Figure 2a). Therefore, despite the different behavior of the two covalent structures, the VB population analysis will predict very similar covalent-ionic weights for the two bonds. As such, VB weights by themselves, much like static charges in a heteropolar molecule conceal fundamental information, which can be revealed only through the energy

analysis of the VB wave function as done in Equation (2) above.

The ELF approach: The theory of electron localization functions (ELF) has been described elsewhere^[19,20] and is recalled in the Supporting Information. The aim of the ELF approach is to partition the space occupied by a molecule into definite adjacent regions, called “basins”, which correspond to different chemical objects: atomic cores, bonds, lone pairs, and single electron domains. ELF basins, labeled hereafter as Ω_A , are either core basins that include the nucleus, or valence basins that generally do not include a nucleus (except for bonds containing hydrogen). The synaptic order of a given valence basin is its number of connections to core basins; a disynaptic basin $V(A,X)$ characterizes a two-center covalent bond, while a lone pair $V(X)$ is monosynaptic, etc.

ELF theory calculates the mean populations, $\bar{N}(\Omega)$, of the basins; these populations can be interpreted to arise from weighted VB structures. One may further carry out a statistical analysis of the basins' populations through the covariance matrix, which provides information about electron delocalization. For example, a large covariance matrix element between two basins Ω and Ω' indicates substantial fluctuation of electronic density between these two basins. In particular the diagonal element of the covariance matrix, the variance $\sigma^2[\bar{N}(\Omega)]$ of a basin's population, that is, the square of the standard deviation of the population, is the degree of fluctuation of the given electron pair, which can be interpreted as the dispersion due to VB structures. Scheme 2 summarizes the electron density properties for ideal two-electron bonds of the covalent and ionic types.^[19d,20]



Scheme 2. Expected ELF properties for the ideal covalent and ionic bonds.

Technical notes: VB Calculations: Molecular geometries were optimized by MP2/6-31G* using GAUSSIAN-98.^[28] The VB calculations were done with the Xiamen package.^[27] A basis set of double-zeta + polarization quality was used for all the VB calculations, unless noted otherwise. The 6-31G* basis set was used for the study of A-X bond (A, X = atoms of the second line or heavier), while the 6-31G** was employed for the study of A-H bonds. For heteropolar bonds involving a fluorine atom, we added standard diffuse

functions. In a few cases we repeated the VBCI calculations with larger basis sets, up to cc-pVTZ,^[29] to see the basis set dependence of the bond energy. As a benchmark method we used CCSD(T),^[30] which is known to give reliable bond energies (see Supporting Information).

ELF calculations: The analysis of the ELF function has been carried out with the TopMoD program.^[31] Here too, the 6-31G* basis set and the hybrid Hartree-Fock density functional B3LYP^[32] were used throughout unless noted otherwise. Since the density is correct to second order, the mono-determinantal level is sufficient, and is in anyway compatible generally with higher levels.^[20] We further note that DFT includes correlation implicitly; this and the fact that the definite kinetic energy and the one electron density distribution, in the ELF formula, take into account correlation by construction, mean that the ELF results can be used in conjunction with the VB results, which include electron correlation explicitly. In the C-F and Si-F cases, we have also used a larger basis set including a set of diffuse functions on Si and F (6-31+G*).

Results and Discussion

Valence-bond computational trends: A test of the accuracy (see results in Table S1 in the Supporting Information) of bond dissociation energies, D_e , as calculated by the BOVB and VBCI methods, was performed by using different basis sets, ranging from 6-31G* to cc-pVTZ. These data were compared with the corresponding benchmark CCSD(T) values, and wherever available with experimental values. The two VB methods give similar results, and in all cases the calculated VB values are compatible with the benchmark values, within a few kcal mol⁻¹. Moreover, the VB and CCSD(T) methods exhibit a similar basis set dependence, and with the cc-pVTZ basis set, the values approach the experimental quantities. A test of the dependence of RE_{CS} on method and basis set was also carried out (see results in Table S2 in the Supporting Information). The results show small to moderate dependence, which is expected as most molecular properties show anyway such dependencies. Importantly, what do not depend on method or basis set are the trends in the RE_{CS} quantity.

Covalent, ionic and charge-shift bonds emerge from VB:

Table 1 collects BOVB calculated properties for 21 different single bonds. BOVB calculations constitute our largest and uniform data set. Still, in some cases, where the RE_{CS} values exhibit method dependence, we show also corresponding VBCI data. In each case we show the contribution to the bond dissociation energy due to the lowest structure, either the covalent (D_{COV}) or ionic (D_{ION}), the total bond energy (D_e), the charge shift resonance energy (RE_{CS}), and the weight of the covalent structure (w_{COV}).

In Table 1, entries 1–7, one can see the two classical bond families; Table 1, entries 1–5 correspond to classical covalent

Table 1. Properties of single bonds and their classification according to VB theory.

Entry	Bond ^[a]	D_e	D_{cov}	D_{ion}	RE_{CS}	ω_{cov}	Origin of bonding
1	H–H ^[b]	105.4	93.7	–	11.7	0.760	Cov
2	Li–Li	20.9	15.5	–	5.4	0.810	Cov
3	H ₃ C–H ^[b]	105.7	90.2	–	15.4	0.694	Cov
4	H ₃ Si–H ^[b]	93.6	82.5	–	11.1	0.648	Cov
5	H ₃ C–CH ₃	94.7	66.4	–	28.3	0.600	Cov
6	Na–Cl ^[c]	90.7	–	84.3	6.4	0.285	Ion
7	Na–F ^[d]	102.5	–	101.9	0.6	0.070	Ion
8	F–F ^[a]	36.2	–30.5	–	66.7	0.728	CS
	F–F ^[c]	32.3	–21.8	–	54.1	0.741	CS
9	Cl–Cl ^[a]	40.0	–21.9	–	61.9	0.684	CS
	Cl–Cl ^[c]	41.6	–3.4	–	45.0	0.661	CS
10	Br–Br ^[a]	41.3	–18.1	–	59.4	0.713	CS
	Br–Br ^[c]	44.1	+9.2	–	34.9	0.667	CS
11	F–Cl ^[a]	47.9	–39.7	–	87.6	0.588	CS
	F–Cl ^[c]	49.3	–29.8	–	79.1	0.585	CS
12	F–Br	50.1	–34.5	–	84.6	0.554	CS
13	Cl–Br	40.0	–9.2	–	49.2	0.694	CS
14	HO–OH ^[a]	50.8	–11.7	–	62.5	0.676	CS
	HO–OH ^[c]	49.8	–1.1	–	50.9	0.673	CS
15	H ₂ N–NH ₂ ^[a]	68.5	19.6	–	48.9	0.612	CS
	H ₂ N–NH ₂ ^[c]	70.5	35.7	–	34.8	0.675	CS
16	H–F ^[c,e]	134.0	49.3	–	84.7	0.551	CS
17	H ₃ C–F ^[c]	99.2	28.3	–	70.9	0.450	CS
18	H ₃ C–Cl ^[f]	79.9	34.0	–	45.9	0.616	CS
19	H ₃ Si–Cl	102.1	37.0	–	65.1	0.572	CS
20	H ₃ Ge–Cl ^[g]	88.6	33.9	–	54.7	0.587	CS
21	H ₃ Si–F ^[c]	140.4	–	103.8	36.6	0.358	ion-CS

[a] SD-BOVB calculation in 6–31G* basis set, unless specified otherwise. [b] 6–31G**. [c] VBCISD followed by Davidson correction. [d] From ref. [7b]. [e] 6–31 + G*. [f] From ref. [7c]. [g] From ref. [7d].

bonds, for which the bond energy is dominated by the spin-pairing contribution in the covalent structure, while Table 1, entries 6 and 7 correspond to the classical ionic bonds, in which bonding is dominated by the electrostatic energy in the ionic structure. *In both classical groups the charge-shift resonance energy is a minor bonding effect compared with the principal contributions.*

Alongside the classical groups, we see in Table 1, entries 8–20 a group of bonds where now the classical covalent or ionic interactions contribute only weakly, if at all, to the overall bonding energy. The bonding, in this group, arises mainly or solely from the CS resonance energy. This is the group of charge-shift bonds (*CS bonds*), which is seen to include a variety of *homonuclear bonds*, for which the weight of the covalent structure is very similar to those in the covalent-bond family. Notably, almost all dihalogens (Table 1, entries 8–13) display a *negative* bonding energy for the covalent component, corresponding to a repulsive covalent curve as shown in Figure 2b for the F₂ molecule. Moreover, since the covalent structure is calculated at the VBCISD level with dynamic correlation, and since *it remains repulsive* at this level in F–F, Cl–Cl, etc., this means that *dynamic correlation, by itself, cannot create bonding in the covalent structure* of F–F, Cl–Cl, etc. By contrast, the inclusion of the ionic VB structures in the wave function, at both the BOVB and VBCI computational levels, contributes large RE_{CS} quantities and causes a drastic change, leading thereby to significant bond energies. As we noted in the Methods section, the weight of a repulsive covalent structure will be

dominant in all the homopolar bonds, since it is the lowest VB structure in the corresponding wave functions. The feature that distinguishes classical covalent from the CS bonds is the RE_{CS} quantity.

It appears therefore that, in the CS-bonded family of molecules, the only physical interaction that holds the bonded atoms together is the charge-shift resonance energy due to the covalent-ionic fluctuation; again, the term “fluctuation” refers to the deviation of the pair density from the average of one electron per atom (fragment). This conclusion carries over to the O–O bond (Table 1, entry 14), and in tempered manner also to the N–N bond, where the CS resonance energy plays a dominant role. In addition, some regular tendencies are observed in the homonuclear bonds: the CS resonance energies increase, and the covalent interactions become more repulsive, as one moves in a family from bottom to top (Br–Br to F–F), or from left to right in a row (H₂N–NH₂, HO–OH, F–F) of the periodic table. As such, large resonance energies and repulsive covalent interactions seem to be associated with *compact orbitals and the presence of lone pairs*; this observation will turn out to be fundamental.

Alongside the homonuclear bonds, one finds highly polar bonds, such as H–F, Si–Cl, and Ge–Cl, in which the covalent contribution to bonding is inferior to the CS resonance energy. Finally, the Si–F bond (Table 1, entry 21), with a resonance energy of 36.6 kcal mol^{–1}, is a borderline case, in between the charge-shift and ionic families. Clearly therefore, CS bonding transcends ionicity or covalency of the bond, in

the static sense of charge distribution or in terms of weights of covalent and/or ionic contributions to the bond; *the bonding arises rather from the resonance energy due to the covalent-ionic fluctuation of the electron pair density.*^[33]

ELF results and the emergence of covalent, ionic, and charge-shift bonding: Table 2 collects the ELF results for the same group of single bonds. For covalent and CS bonding, we show the population of the disynaptic basin that corresponds to the A–X bond, $\tilde{N}[V(A,X)]$, its variance σ^2 , which is a measure of the charge density fluctuation of the bonding electrons, and the main covariance matrix element, $\langle cov(A,B) \rangle$. For ionic bonds (Table 1, entries 6,7), the core population of the most electropositive atom A is reported instead of nonexistent $\tilde{N}[V(A,X)]$.

Once again, we see three groups of bonds. In Table 2, entries 1–5, we find bonds with almost 2.0 electrons in the disynaptic basin, with weak to moderate fluctuation compared to the total population. Following the classification in Scheme 2 these are the classical covalent bonds. A pictorial representation of the various basins for a typical molecule displaying a bond of this type, the C–C bond in ethane, is displayed in Figure 4.

At equilibrium distance (Figure 4a), the molecule exhibits a disynaptic basin (green) that characterizes the C–C covalent bond with the population of 1.81 e (see entry 5 in Table 2). As one stretches the C–C distance, the disynaptic C–C basin transforms into a pair of monosynaptic basins (orange, Figure 4b), which characterize the dissociated bond; now, each CH₃ fragment bears an unpaired electron.

In entries 6 and 7 of Table 2, we show two bonds that do not exhibit any disynaptic basin, but rather the bare core

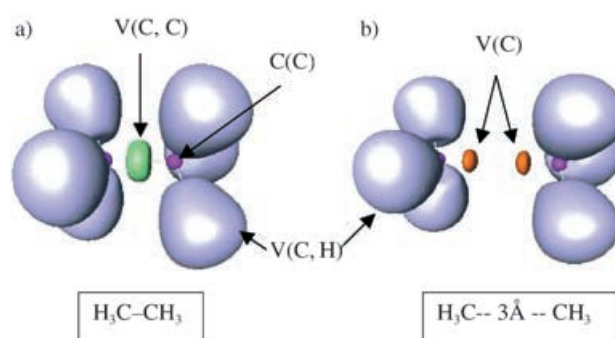


Figure 4. Localization domains in ethane: a) $R_{C-C} = 1.53$ Å. b) $R_{C-C} = 3.0$ Å. Color code: orange: monosynaptic, V(C); green: disynaptic, V(C,C); lilac: disynaptic V(C,H); magenta: core.

basin of the electropositive atom and a monosynaptic basin on the most electronegative one. The population of the core basin of the sodium atom is close to 10 e, and the variance is rather small (0.11–0.12); following Scheme 2 these are classical ionic bonds.

The largest group in Table 2 corresponds to entries 8–17. In all of these bonds the population of the A–X basin is of the order of 1 e[−] or less, and the variances of these populations are large, almost of the same order as the population. The small populations of the disynaptic basins indicate that *these are not classical covalent bonds*, in which two spin-paired electrons are expected to provide the bonding. This is most visible in F–F, which is shown in Figure 3 to possess a disynaptic basin (green) *that exhibits minimal electron pair localization* in the middle of the “bond”, fundamentally different from the barrel-shaped disynaptic basin of the C–C bond in Figure 4a, more akin to the dissociated bond in Figure 4b. In fact, at higher levels of calculations,^[20] in the cases of F–F and Cl–Cl, the disynaptic basins are split into two monosynaptic ones that are 0.2 Å apart, and the electrons in the bonding region behave as though the bonds were “dissociated” with significant Pauli repulsion. This, together with the large variance, signifies that the bonding in these molecules is dominated by fluctuation of the charge density.

This last group of bonds corresponds therefore to the same CS-bonding type that emerges from the VB calculations. As we mentioned in the introductory section, the special nature of the F–F bond emerges also from other density-based approaches.^[17b,21a,21c] Thus, as

Table 2. Populations $\tilde{N}(\Omega)$, population variance σ^2 and summed nonbonded covariance matrix elements $\langle cov(A,B) \rangle$ of ELF basins.

Entry	Molecule	Basin	$\tilde{N}(\Omega)$	σ^2	$\langle cov(A,B) \rangle^{[a]}$	Bond type
1	H–H	V(H,H)	2.0	0.0		cov.
2	Li–Li	V(Li,Li)	2.0	0.17		cov.
3	CH ₄	V(C,H)	1.97	0.63		cov.
4	SiH ₄	V(Si,H)	2.0	0.46		cov.
5	C ₂ H ₆	V(C,H)	2.0	0.63	−0.18	cov.
		V(C,C)	1.81	0.96		cov.
6	NaCl	C(Na)	10.02	0.11		ion.
7	NaF	C(Na)	10.01	0.12		ion.
8	F ₂ ^[b]	V(F,F)	0.44	0.42	−0.49	CS
9	Cl ₂ ^[b]	V(Cl,Cl)	0.73	0.59	−0.38	CS
10	Br ₂	V(Br,Br)	0.81	0.68	−0.40	CS
11	FCl	V(F,Cl)	0.39	0.35	−0.51	CS
12	FBr	V(F,Br)	0.28	0.26	−0.53	CS
13	ClBr	V(Cl,Br)	0.67	0.54	−0.40	CS
14	H ₂ O ₂	V(O,O)	0.49	0.41	−0.43	CS
15	N ₂ H ₄	V(N,N)	1.16	0.77	−0.29	CS
16	HF	V(H,F)	1.22	0.68	−0.64	CS
17	CH ₃ F	V(C,F)	0.86	0.64	−0.28	CS
18	SiH ₃ Cl	V(Si,Cl)	1.55	0.95	−0.18 (−0.63) ^[c]	cov-CS
19	SiH ₃ F	V(Si,F)	0.27	0.24	−0.24	ion-CS

[a] $\langle cov(A,B) \rangle = \langle cov(\tilde{N}[V(A)], \tilde{N}[V(B)]) \rangle + \sum_{X \neq A} \sum_{Y \neq B} \langle cov(\tilde{N}[V(A,X)], \tilde{N}[V(B,Y)]) \rangle$. [b] V(F, F) and V(Cl, Cl)

are the unions of two monosynaptic basins. [c] The value in parentheses is covariance matrix element between V(Si,Cl) and V(Cl).

noted by Bader and Essen,^[17b] in F_2 , the electrons remain localized near the nuclei, the interaction in the binding region is more typical of closed-shell species, and the covalent interaction (due to exchange) is weak. Similarly, a recent density analysis by Rincon and Almeida,^[21e] using *inter alia* VB type wave functions, led to the following conclusion: “ F_2 , Cl_2 , ... show a dominant covalent character but not a shared typed interaction behavior”.

An additional indication of the CS-bonding behavior is provided by the summed elements of the covariance matrix between the $V(A, X)$ and $V(X)$ basin populations; the sums are large and negative. In dihalogen molecules the large negative covariance matrix element between $V(A)$ and $V(B)$ means that a significant quantity of electronic density fluctuates back and forth from one atom to the other, and corresponds to the charge-shift scheme $A^+B^- \leftrightarrow A^-B^+$.

The VB results for H_3Si-Cl show that the bond is clearly a charge-shift type (entry 19, Table 1), but the ELF properties of this bond are less clear-cut (entry 18, Table 2). A source for this difference between the analyses could lie in the exceptionally small ionic radius of the SiH_3^+ ion (actually smaller than that of the CH_3^+ ion, see Figure 7 below),^[7c] which could make a disynaptic basin very difficult to distinguish from a monosynaptic one.

The last entry in Table 2 corresponds to the $Si-F$ bond. With the 6-31G* basis set this bond does not possess a disynaptic $V(Si, F)$ basin. Adding diffuse functions to the basis set (6-31+G*), leads to an emergence of a disynaptic $Si-F$ basin, with a weak population, and large variance, mostly due to the delocalization involving the fluorine lone pairs. Thus, the improvement of the basis set increases the covalent contribution at the expense of the static ionic one, and confirms that although this bond has high static ionicity, it is a borderline case fitting in between the groups of ionic bonds and charge-shift bonds.

Comparison of CS bonding in VB and ELF theories: The match between the predictions of the two methods is good. However, it is most vivid in the homonuclear bonds that for all intents and purposes would be considered “purely covalent” by the traditional bond classification *based on static charge distribution*. To project this unified prediction of the two methods, Figure 5 shows a plot of the basin population for homonuclear bonds vis-à-vis the charge shift resonance

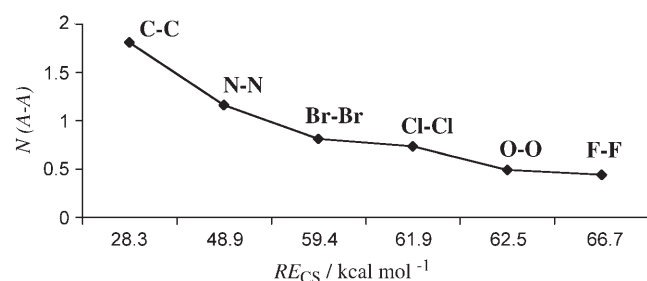


Figure 5. A correlation between the population of the disynaptic basin, calculated by ELF, and the charge-shift resonance energy, calculated by VB, in a series of homonuclear bonds.

energy. The correlation is apparent; the smaller the basin population the larger the charge-shift resonance energy. Recalling (Table 1) that all these bonds have very similar weights of covalent and ionic contributions to bonding, it is clear that the major feature of bonding that distinguishes this group is the RE_{CS} quantity that arises from the covalent-ionic fluctuation of the pair density.

The correlation in Figure 5 indicates that both theories converge to the same conclusion, thereby substantiating the classification of CS bonding as a distinct bonding-type that is supported by a dominant RE_{CS} quantity, due to covalent-ionic fluctuation. Furthermore, both theories show that *this group of bonds transcends considerations based on static charge distribution, and is more concerned with the “dynamic bond ionicity”*.^[34]

Origins of CS bonding

While the phenomenon of CS bonding is derived from two independent theoretical treatments, still one would like to base this bonding type on some fundamental principles. The following sections relate the phenomenon to fundamental properties of atoms and bonding mechanisms.

The lone-pair bond weakening effect: In bonds such as $F-F$, $Cl-Cl$, $O-O$, etc, the spin-pairing leads to a covalent structure that is either destabilized or only weakly stabilized relative to the dissociated atoms (Table 1). This failure of the covalent structure to provide significant bonding was quantified before in VB terms,^[7a-f] and found to originate primarily in *the repulsion between the bonding electrons and the lone pairs that have the same symmetry as the bond*, the repulsion between the lone pairs themselves makes a lesser contribution.^[7f]

The role of this repulsive interaction is well accepted.^[21,35] Sanderson^[35] has referred to this interaction as the lone-pair bond-weakening effect (LPBWE), and has demonstrated its importance for all atoms bearing electron pairs. For example, in the case of the $F-F$ bond, the LPBWE amounts to $75.3 \text{ kcal mol}^{-1}$ at equilibrium distance;^[7f] the repulsion overcomes the stabilization due to spin pairing, *and is responsible fully for the repulsive nature of the covalent interaction in this molecule* (e.g. see Figure 2b). The LPBWE is not restricted to $F-F$ and will be common to all bonds between fragments X that carry σ -type lone pairs, for example, F , Cl , Br , I , OH , SH , SeH , NH_2 , PH_2 , SbH_2 , etc. The covalent structures in such $X-X'$ bonds, will be either weakly bonding or repulsive. Moreover, the LPBWE will carry over, albeit to a smaller extent, to heteronuclear $A-X$ bonds, when only one of the fragments carries a σ -lone pair. According to VB theory, in such bonds, the bonding will have to be sustained by the RE_{CS} quantity that arises from the covalent-ionic fluctuation of the electron-pair density; the spin pairing in the covalent structure will make either a small contribution or altogether a negative contribution to the bonding energy. The discussion that follows provides the fundamental reason why must RE_{CS} be large in these bonds.

The atom compactness and electron-pair richness effects:

What are then the origins of the large CS resonance energy? And when do we expect it to be large? Some guiding insight into these questions can be gained from Figure 6, which shows a plot of the RE_{CS} quantity against the sum of the electronegativities of the two atoms that constitute the bond. Figure 6a shows this plot only for the homonuclear bonds, A–A. One can see two families on two different lines. The first line involves hydrogen and atoms of the first row of the periodic table, that is, atoms of comparable size. The second family involves corresponding atoms of lower rows of the periodic table. More lone-pairs on the atoms seem to play the same role, and for example, Br–Br and Cl–Cl exhibit larger RE_{CS} compared with the N–N bond that carries less lone-pairs.

Figure 6b is a similar plot for all the bonds in this study, labeled generally as A–X. Despite the scatter, the general trend is basically similar to the plot in Figure 6a; the larger the sum of electronegativities and the more lone-pair rich are the atoms the greater is the CS resonance energy of the bond. The scatter in the plot reflects, in part, the effect of the electronegativity difference, namely the classical Pauling effect on the covalent-ionic resonance energy.^[9] Thus, for a given electronegativity sum ($\chi_X + \chi_A$), the RE_{CS} quantity increases, to some extent, with increase of the electronegativity difference ($\chi_X - \chi_A$), thereby reflecting an increase of RE_{CS} due to the stabilization of the ionic structure, A^+X^- , and its stronger mixing into the covalent structure. However, the electronegativity difference constitutes only a secondary influence. Indeed, in contrast to the behavior in Figure 6b where a general correlation with ($\chi_X + \chi_A$) is apparent, no correlation whatsoever is observed when the RE_{CS} data is plotted against ($\chi_X - \chi_A$) alone in Figure 6c. *The fundamental correlation is with the sum of electronegativities.*

Similar findings were noted before^[7e] for the charge-shift resonance energy of π bonds, and the respective plot is adopted here in Figure 6d. Thus, here too, the charge-shift resonance energy was found^[7e] to be large for atoms that are either highly electronegative (O, N) and/or moderately electronegative but bearing electron pairs (S, P). Clearly, the CS resonance energies of σ and π bonds, be they homonuclear or heteronuclear, exhibit a uniform behavior; in both cases, *the dominant factor is the sum of the electronegativities and/or the number of lone-pairs on the constituent atoms.*

Another interesting dependence of the CS resonance energy is on the compactness of the orbital that participates in bonding. Indeed, as we showed in an earlier treatment,^[7b] the effect of orbital compactness can be modeled by calculating the CS resonance energy of an H'_2 molecule, where H' is an atom with a variable orbital exponent, ζ . The approximate relationship given in Equation (4) was found.

$$\ln(RE_{CS}) \approx 8.9 \log_e(\zeta) - 0.4 \quad (4)$$

Thus as ζ increases, the orbital of H' becomes more compact, and the CS resonance energy increases. This relationship provides a simple explanation for the dependence of RE_{CS} on the electronegativity sum in Figure 6. The sum of electronegativity is an index of compactness of the valence orbitals^[36,37] of the constituent atoms of the bond, and the correlation in Figure 6a,b reflects therefore the compactness of the atoms that participate in the bond.

While this relationship accounts for one feature of the CS resonance energy, it does not account for the effect of lone-pair richness. To understand the latter, we first need to consider the fundamental changes that occur during bond making,^[17b,c,21a,21c,38] based on the virial theorem expressed in Equation (5a), where E is the total energy, V and T are respectively the potential and kinetic components, and R is

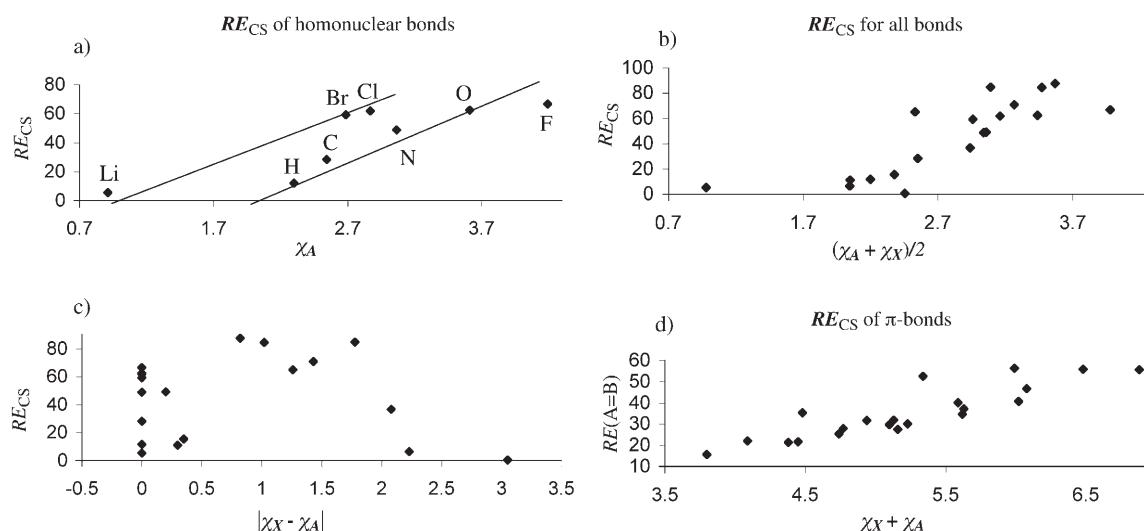


Figure 6. Correlation between the charge-shift resonance energy (RE_{CS}) of a bond and the electronegativity sum of the constituent fragments in: a) homonuclear bonds, and b) all bonds in Table 1. c) Note the lack of correlation between RE_{CS} and the electronegativity difference for the bonds in (b). d) A correlation between the RE_{CS} of π bonds and the sum of electronegativities.

the interatomic distance between the two atoms (or fragments).

$$-RdE/dR = 2T + V \quad (5a)$$

The term on the left of Equation (5a; the force acting on the molecule multiplied by the respective bond length, R) is zero at equilibrium, that is, for $R = R_{eq}$. This means that any properly optimized wave function at its own equilibrium distance R_{eq} must obey the virial ratio of the kinetic to the potential energy given in Equation (5b).

$$2T/(-V) = 1 \quad (5b)$$

Achieving this ratio results in energy lowering, namely in bonding, which is expressed in Equation (5c).

$$\Delta E = -\Delta T = 0.5 \Delta V; (\Delta V < 0) \quad (5c)$$

However, far from equilibrium, the virial ratio ($2T/(-V)$) will be off-balance: larger than unity for $R < R_{eq}$ (i.e. the kinetic energy T being too large to satisfy Equation (5b)), and smaller than unity for $R > R_{eq}$.^[38g]

Let us now bring together two atoms (fragments): At infinite separation the atoms (fragments) obey individually the virial ratio [Eq. (5b)]. Simply shortening the distance, without any other change, will cause a decrease of the kinetic energy, and will thereby put the virial ratio of the species off-balance.^[38d,e,g] The wave function will then have to relax in some way to restore this ratio and decrease the total energy. At the purely covalent level, this is accomplished by orbital shrinkage,^[38d] which lowers the potential energy but raises the kinetic energy steeply. At the optimal distance of the covalent structure, R_{eq}^{cov} , the virial ratio will be obeyed. However, the purely covalent wave function yields, as a rule, too small bonding energies and bonding distances that are too long relative to accurately calculated spectroscopic parameters; this wave function is insufficient. To optimize the bonding, *the orbital shrinkage mechanism has to be augmented by an additional mechanism*. This mechanism allows the wave function to include ionic structures, thereby resulting in an optimized covalent-ionic wave function Ψ_{A-X} with a shorter equilibrium distance R_{eq}^{A-X} , where the virial ratio is obeyed. At this distance, which is shorter than R_{eq}^{cov} , the covalent component of the wave function no longer obeys the virial ratio, which now exceeds unity, and it is the mixing of the ionic structures that restores the ratio to unity. Therefore, it is clear that the effect of ionic structures is to diminish the $2T/(-V)$ ratio, that is, to reduce the excess of kinetic energy relative to potential energy.

Thus, CS resonance due to the mixing of ionic structures into the covalent one is expected to be responsible, along with orbital shrinkage, for the adjustment of the kinetic and potential energy terms to the virial ratio at equilibrium. This effect of the CS resonance was ascertained by us using BOVB calculations.^[39] The following trends were found for H_2 at equilibrium distance: 1) upon binding, the orbitals

shrink, 2) the shrinkage of the orbitals in the covalent structure lowers the potential energy, V , but excessively raises the kinetic energy, T , thereby tipping the virial ratio off-balance; and 3) adding the ionic structures lowers T without having much an effect on V , thus restoring the correct virial ratio.^[39] Generalizing to typical *classical covalent bonds*, like H–H or C–C bonds, the mechanism by which the virial ratio is obeyed during bond formation is primarily orbital shrinkage, and therefore the charge-shift resonance energy is only a small corrective effect.

Let us now consider a bond that bears adjacent electron pairs, as in F_2 , Cl_2 , etc. The presence of lone pairs creates additional Pauli repulsions (LPBWE), which raise the kinetic energy.^[38b] An extreme case is that of the F_2 molecule, in which the covalent component of the bond is repulsive, having excessive kinetic energy throughout, thus making the virial ratio greater than unity at any distance in the covalent wave function. Therefore, by reference to H_2 , which lacks these repulsive interactions, the additional increase of kinetic energy brought by LPBWE must be compensated by greater participation of covalent-ionic mixing. Moreover, the necessity for large RE_{CS} is further reinforced by the fact that the atoms that bear lone pairs are also compact, and shrinkage of a compact atom (fragment) raises its kinetic energy more steeply than in a case of a diffuse atom (fragment).^[40] It follows therefore, from the above discussion, that *the smaller the atom (fragment) and the more lone-pair rich it is, the larger will be the excess kinetic energy, in the covalent structure, and the greater RE_{CS} would be required to restore the virial ratio*. This is the reason why the homonuclear bonds of F, O, N, Cl, etc., are CS bonds, and why many heteronuclear bonds containing F, Cl, O, S, N, P, will have a propensity for CS bonding. This is also the reason why the RE_{CS} peaks for F, which is the most compact and lone-pair rich atom in its period. This property comes inherently with the atom (fragment). It follows therefore that *CS bonding is the outcome of a fundamental mechanism of bonding*.

Manifestations of CS bonding

This section links the concept of CS bonding to some experimental manifestations.

CS bonding and experimentally derived bond densities: The density difference in the bonding region,^[18] so-called also the “bonding density” is defined as Equation (6), where ρ_M is the electron density of the molecule, ρ_{Pro} is the density of the pro-molecule, which consists as the superimposed density of the two non-interacting atoms at the equilibrium bond distance.

$$\Delta\rho(B) = \rho_M - \rho_{Pro} \quad (6)$$

Thus, ρ_{Pro} serves as a reference density to quantify the nature of charge reorganization in the molecule relative to the nonbonded atoms. For H_2^+ and H_2 , $\Delta\rho(B) > 0$, namely charge density accumulates in the bonding region and acts

as the “glue” that binds the atoms. This simple bonding paradigm, and its articulation based on the Hellman–Feynman theorem,^[41,42] have created an incentive to quantify the $\Delta\rho(B)$ quantity by experimental X-ray and neutron diffraction techniques.^[43] The findings of these studies led to two types of “covalent bonds”. In the first type, there were bonds like Li–Li, C–C, Si–Si, C–H, etc for which the $\Delta\rho(B)$ quantity was positive much like in the H_2 molecule. However, the other type exhibited $\Delta\rho(B)$ that was negative or marginally positive. Among the latter class of “covalent bonds” were the bonds, F–F, Cl–Cl, O–O, S–S, N–N, N–O, C–F, and C–O.

We fully agree with the judgement that^[21b–d] that the negative bonding density is an artifact of the choice of the pro-molecule, however, the depleted density or the virtual lack of a clear bonding basin are not artifacts, since these latter features result also from examination of the density without resort to the pro-molecule reference (e.g., Figure 3). We note that the classification of two covalent bond groups based on their electron density can be connected to the central notion in the present paper, of classical covalent bonding versus CS bonding. Right at the outset, one can identify that the first group of bonds, for example, C–C, Si–Si, C–H, that possess significantly positive $\Delta\rho(B)$, consists of classical covalent bonds, while the second group, for example, F–F, O–O, Cl–Cl, C–F, which possesses depleted $\Delta\rho(B)$ consists of the group of CS bonds. The depletion of electron density from the bonding region is diagnostic of poor binding by the spin-pairing interaction of the covalent structure, due to LPBWE effect. As a consequence of the LPBWE, the electrons try to avoid these repulsive interactions by polarizing away from the bonding region to the outer-side regions of the bond, leading thereby to depleted bonding density (see Figure 3 for the ELF domains). As discussed above, the bonding interaction is provided by the covalent-ionic fluctuation of the pair density. This covalent-ionic fluctuation does not lead to electron density build-up in the bonding region, and is more typical of closed-shell interaction, as indeed probed by the various other electron density criteria.^[17b,20,21e]

CS bonding and the rare ionic chemistry of silicon in condensed phases: A large CS resonance energy typifies also bonds with a high static ionicity, like H–F, C–F, Si–F, Si–Cl, and Ge–Cl (Table 1). This arises due to a combination of effects, one being the LPBWE of the lone-pair bearing heteroatom, and the second is the strong covalent-ionic interaction due to the decreased energy gap between the two structures.^[7] In the case of Si–X bonds, the ionic VB structure undergoes a special stabilization that can be appreciated from the calculated charge distribution of the ionic structures, in Figure 7, for Si–Cl versus C–Cl.^[7c,d] It is seen that the positive charge of H_3Si^+ is concentrated on silicon, while in the case of CH_3^+ the charge is delocalized over all the atoms, placing only a small charge on the carbon. This in turn causes much stronger electrostatic interactions in the ionic structure $H_3Si^+Cl^-$ compared with $H_3C^+Cl^-$. The

result is that the minimum of the ionic curve becomes very deep for $H_3Si^+Cl^-$ and it coincides with the minimum of the covalent structure, leading thereby to a strong covalent-ionic mixing and large RE_{CS} compared with the carbon analogue (65 versus 46 kcal mol^{−1}, see Table 1). The same situation carries over to any R_3Si-Cl versus R_3C-Cl , R =alkyl, etc; in each case the $R_3Si^+Cl^-$ structure will have a minimum coincident with the covalent structure and a large resultant RE_{CS} , some 21 kcal mol^{−1} larger than that of the carbon analogue.^[7c,d,44] In a condensed phase, the ionic structure is stabilized by the environment, but since the Si^+Cl^- minimum is tight, the stabilization will be only moderate, and hence, the ionic curve should remain close to the covalent curve, thereby retaining the large RE_{CS} interaction of the bond. Thus, in a condensed phase, the covalent-ionic mixing remains large giving rise to Si–X bonds that stay intact due to the large CS resonance energy. Since the heterolysis of the Si–X bond would result in a loss of this resonance energy, solvolysis of the bond would necessarily be difficult. This, in our view, is one of the reasons why it was so difficult to generate “free” silicenium ions in condensed phases,^[13,15] by contrast to carbon chemistry which is replete with carbocations.^[14] Other reasons were discussed before^[7d] and are associated with the fact that the positive charge on the silicon in a silicenium ion is screened by the negative charge of the substituents (Figure 7). This leads to inefficient solvation of the free silicenium ion, on the one hand, and on the other, to the propensity of silicon to form hypercoordinated species, with directed Si–X bonds in which bonding is sustained by large CS resonance energy.^[45] Indeed, hypercoordination abounds in the chemistry of silicon.

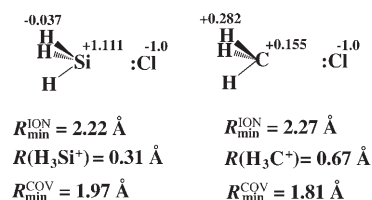


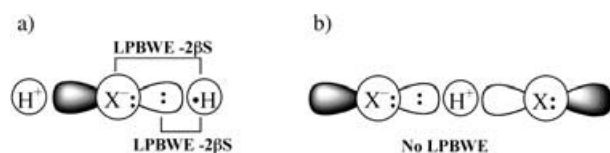
Figure 7. Coulson–Chirgwin charges and some geometric parameters of the ionic structures $H_3C^+Cl^-$ and $H_3Si^+Cl^-$.

The R_3Si-F bond is a limiting case. On the one hand, the presence of F creates propensity for CS bonding, but on the other hand, the small size of the silicenium ion intensifies the Coulomb interactions with F^- , and causes the ionic structure to be much lower in energy than the covalent structure (Table 1), thus preventing an overly large value of the resonance energy RE_{CS} . The RE_{CS} quantity will diminish gradually in a series of heteropolar bonds as the ionic structure gets further and further stabilized relative to the covalent structure, until the interaction between the two structures becomes too small to matter. This limit occurs in the classical ionic bonds, such as Na^+F^- , where the covalent-ionic gap is too large to lead to any appreciable RE_{CS} .

Other manifestations of CS bonding: We would expect to see manifestations of CS bonding on reactivity for cases which involve cleavage of CS bonds. Our preliminary studies^[46] show that the loss of CS resonance energy is the root cause of the computational^[47] and experimental^[48] findings that halogen transfer reactions (and especially of fluorine) [Eq. (7a)], have much larger barriers (by $>20 \text{ kcal mol}^{-1}$ for $X=F$) than the corresponding hydrogen transfer processes [Eq. (7b)].



The two processes have almost identical covalent structures, but they differ in the status of the ionic VB structures in the vicinity of the transition state. In reaction (7a), the key combination of ionic structures, $\text{H}^\cdot \text{X}^\cdot \leftrightarrow \text{H}^+ \text{X}^\cdot$, is destabilized by two repulsive three-electron interactions^[49] between H^\cdot and the X^\cdot fragment (Scheme 3a). By



Scheme 3. Lone-pair bond weakening effect (LPBWE) in the ionic structure for X-transfer reactions and the lack of LPBWE in the ionic structure of H-transfer reactions. The $-2\beta\text{S}$ terms correspond to the repulsion energy of the particular interaction.

contrast, the ionic combination $\text{X}^\cdot \text{H}^+ \text{X}^\cdot \leftrightarrow \text{X}^\cdot \text{H}^+ \text{X}^\cdot$, for Equation (7b), is devoid of repulsive interactions (Scheme 3b versus 3a). The destabilization of the ionic structure during X-transfer results in a loss of RE_{CS} in the respective transition state. Since the $\text{H}-\text{X}$ bonds, and especially $\text{H}-\text{F}$, have large RE_{CS} to begin with, the loss is significant and the barrier is higher for the X transfer reaction and especially so for $X=F$. Similar trends were recently reported also for group transfer reactions in lanthanide complexes.^[50]

Scope and territory of CS bonding: The territory of CS bonding for electron pair bonding is ultimately larger than discussed in this paper. Thus, a recent VB study^[51] shows that coordinate bonding such as the one between tetravalent boron and amines, $\text{R}_3\text{B}-\text{NR}'_3$, is dominated by CS resonance energy. Similarly, Coote et al.^[52] found that the dependence of the relative bond strengths of $\text{R}-\text{X}$ bonds ($\text{R}=\text{Me}$, Et , $i\text{Pr}$, tert-Bu ; $\text{X}=\text{H}$, F , OH , OCH_3) follows the CS resonance energy. Our recent study of $\text{M}-\text{H}$ bonds, where M is a first-row transition-metal,^[53] showed that the CS resonance energy is quite significant despite the apparent “covalency” of most of the bonds. Furthermore, RE_{CS} was found to increase from left to right in the period, and to be affected by the presence of the $2\text{s}^2 2\text{p}^6$ core electron pairs, which behave as lone-pairs on an atom. The above analyzed propensity of atoms (fragments) to generate CS bonding suggests that

many of the bonds of first-row transition metals will tend to be CS bonds, especially when the bonding partner an electronegative and/or lone-pair rich atom. More such CS bonds should be looked for among the bonds between the heavier elements of the periodic table. CS bonding typifies also the bonds of noble gas atoms, for example, XeF_n ($n=2,4,6$), and all hypercoordinated species,^[54] such as PCl_5 , SF_n ($\text{F}=4,6$), and so on. CS bonding is expected to be ubiquitous with a large territory waiting to be explored.

Concluding Remarks

This study uses valence bond (VB) theory and electron-localization function (ELF) calculations to demonstrate that along the two classical bond families of covalent and ionic bonds, which describe the electron-pair bond, there exists a distinct class of charge-shift bonds (CS bonds) in which the fluctuation of the electron pair density plays a dominant role. In VB theory, this is manifested by large covalent-ionic resonance energy, RE_{CS} , and in ELF, by a depleted basin population with a large variance and negative covariance.

The large RE_{CS} quantity of CS bonds was shown to be an outcome of the mechanism necessary to establish equilibrium and optimum bonding during bond formation. As atoms (fragments) bind they shrink, and hence, the steep increase in their kinetic energy exceeds the lowering of the potential energy that results from the diminished atomic size. The kinetic energy rise becomes all the more severe when the atoms (fragments) bear lone-pairs, which by repulsion with the bonding electrons and between themselves further augment the kinetic energy during binding. The RE_{CS} quantity constitutes therefore *the energy mechanism required to lower the excess kinetic energy, so that the total energy of the molecule can ultimately decrease*. Heuristically speaking, the electrons in the bonding region trade off their frantic “motions” near the atoms by the slower fluctuations between the atoms.

Atoms (fragments) that are prone to CS bonding are compact electronegative and/or lone-pair-rich species, albeit with moderate electronegativity; the CS-property peaks at fluorine. Indeed, CS bonding was found to include the following bond groups: a) Homopolar σ and π bonds of heteroatoms with zero static ionicity. b) Heteropolar σ and π bonds of the electronegative elements ($\text{F}-\text{Cl}$, $\text{F}-\text{Br}$). c) Heteropolar σ and π bonds of the electronegative elements (F , O , N , Cl) to H and C . d) Heteropolar bonds, with large static ionicity, of second and third row metalloids (Si , Ge , Sn , etc) to electronegative and electron-pair rich atoms (e.g., F , Cl). e) All hypercoordinate molecules have CS bonding.^[54] Our most recent results show that triple bonding is almost invariably CS bonding. Clearly, *this is a distinct and large group of bonding that transcends consideration of covalency or static charge distribution*.

In sum: CS bonding is ubiquitous; defining its territory and manifestations will ultimately depend on the acceptance of the idea and its articulation by experimentalists and theoreticians.

Acknowledgements

S.S. is thankful to T. Ziegler, D.G. Truhlar, and R. Bader for helpful comments and discussion.

- [1] G. N. Lewis, *J. Am. Chem. Soc.* **1916**, 38, 762.
- [2] W. Heitler, F. London, *Zeits. für Physik.* **1927**, 44, 455.
- [3] L. Pauling *The Nature of the Chemical Bond*, Cornell University Press, Ithaca, New York, **1939** (3rd ed, **1960**).
- [4] J. C. Slater, *J. Chem. Phys.* **1965**, 43, S11.
- [5] For a recent new insight from partition of bonding energies using an energy decomposition analysis,^[6] see: a) A. Kovacs, C. Esterhuysen, G. Frenking, *Chem. Eur. J.* **2005**, 11, 1813; C. Esterhuysen, G. Frenking, *Theor. Chem. Acc.* **2004**, 111, 381; b) F. M. Bickelhaupt, E. J. Baerends, *Rev. Comput. Chem.* **2000**, 15, 1.
- [6] For the Morokuma and Ziegler–Rauk schemes see: K. Kitaura, K. Morokuma, *Int. J. Quant. Chem.* **1976**, 10, 325; T. Ziegler, A. Rauk, *Theor. Chim. Acta* **1977**, 46, 1.
- [7] a) G. Sini, P. Maitre, P. C. Hiberty, S. S. Shaik, *J. Mol. Struct.* **1991**, 229, 163; b) S. Shaik, P. Maitre, G. Sini, P. C. Hiberty, *J. Am. Chem. Soc.* **1992**, 114, 7861; c) D. L. Lauvergnat, P. C. Hiberty, D. Danovich, S. Shaik, *J. Phys. Chem.* **1996**, 100, 5715; d) A. Shurki, P. C. Hiberty, S. Shaik, *J. Am. Chem. Soc.* **1999**, 121, 822; e) J. M. Galbraith, E. Blank, S. Shaik, P. C. Hiberty, *Chem. Eur. J.* **2000**, 6, 2425; f) D. L. Lauvergnat, P. C. Hiberty, *J. Mol. Struct.* **1995**, 338, 283.
- [8] a) The use of $RE_{CS}(A-A) \approx 0$ appears as a working assumption, for example, on pages 73–100 (see also footnote 13 on page 73), in L. Pauling *The Nature of the Chemical Bond*, Cornell University Press, Ithaca, New York, **1939** (3rd ed, **1960**), where it is estimated that the ionic structures in, for example, Cl_2 will contribute less than 2% to the total bond energy. A stricter assumption is used in Sanderson's treatment,^[35] which neglects the resonance energy altogether. b) For a heteronuclear bond, $A-X$, the covalent contribution, D_{COV} , to the bonding energy is given by: $D_{COV} = [D_{A-A} \cdot D_{X-X}]^{1/2}$.
- [9] The charge distribution in $A-X$ can be quantified from the electronegativity difference as: $\delta = 1 - \exp[-0.25(\chi_X - \chi_A)^2]$ given in most periodic tables, and appears in L. Pauling *The Nature of the Chemical Bond*, Cornell University Press, Ithaca, New York, **1939** (3rd ed, **1960**), p. 98. See also the relationship $D_{AX} - D_{COV} = 23(\chi_X - \chi_A)^2$, which is the expression for the covalent-ionic resonance energy for a polar bond.
- [10] For pioneering localization methods, see: C. Edmiston, K. Ruedenberg, *Rev. Mod. Phys.* **1963**, 35, 457; C. Edmiston, K. Ruedenberg, *J. Chem. Phys.* **1965**, 43, 597; S. F. Boys, *Rev. Mod. Phys.* **1960**, 32, 296; J. M. Foster, S. F. Boys, *Rev. Mod. Phys.* **1960**, 32, 300.
- [11] a) B. Silvi, AIM analysis, of SiH_3-F and $Li-F$ using B3LYP/6-31+G* and B3LYP/6-31G* levels; b) R. F. W. Bader, T. T. Nguyen-Dang, *Adv. Quantum Chem.* **1981**, 14, 63;
- [12] For other highly ionic bonds to silicon, see: J. Henn, D. Ilge, D. Leusser, D. Stalke, D. Engles, *J. Phys. Chem. A* **2004**, 108, 9442.
- [13] Y. Apeloig *Theoretical Aspects of Organosilicon Compounds in The Chemistry of Organic Silicon Compounds*, Vol. 1 (Eds.: Y. Apeloig, Z. Rappoport), Wiley, Chichester, England, **1989**, Chapter 2.
- [14] a) For a variety of crystallized carbocationic salts, see: T. Laube, *Acc. Chem. Res.* **1995**, 28, 399; b) A. H. Gomes de Mesquita, C. H. MacGillavry, K. Eriks, *Acta Crystallogr.* **1965**, 18, 437; c) G. K. S. Prakash, S. Keyaniyan, S. K. R. Aniszfeld, L. Heiliger, G. A. Olah, R. C. Stevens, H.-K. Choi, R. Bau, *J. Am. Chem. Soc.* **1987**, 109, 5123; d) For a recent "bottling" of *tert*-butyl cation, see: T. Kato, C. A. Reed, *Angew. Chem.* **2004**, 116, 2968; *Angew. Chem. Int. Ed.* **2004**, 43, 2908.
- [15] a) For a few reviews on the elusive R_3Si^+ ion in condense phases, see: Y. Apeloig, A. Stanger, *J. Am. Chem. Soc.* **1987**, 109, 272; Y. Apeloig, *Stud. Org. Chem.* **1987**, 31, 33; J. B. Lambert, L. Kania, S. Zhang, *Chem. Rev.* **1995**, 95, 1191; b) for a recent exception, see: J. B. Lambert, Y. Zhao, *Angew. Chem.* **1997**, 109, 389; *Angew. Chem. Int. Ed. Engl.* **1997**, 36, 400; K.-C. Kim, C. A. Reed, D. W. Elliott, L. J. Mueller, F. Tham, L. Lin, J. B. Lambert, *Science* **2002**, 297, 825.
- [16] One must not confuse the VB results with the fact that in MO-based theory, F_2 is unbound at the MO level but becomes bound when electron correlation is included by means of configuration interaction (CI). The MO wave function is unbound because it involves excess ionicity (50%)! The CI "cleans" some of the ionicity and creates a more balanced wave function, which leads to some bonding. In the end, in both theories the bonding will arise from the RE_{CS} , however, the physical effect that causes this bonding, is not apparent from the MO-CI procedure.
- [17] a) R. F. W. Bader, *Atoms in Molecules: A Quantum Theory*, Oxford University Press, Oxford, **1990**; b) R. F. W. Bader, H. Essén, *J. Chem. Phys.* **1984**, 80, 1943; c) C. Gatti, P. J. MacDougall, R. F. W. Bader, *J. Chem. Phys.* **1988**, 88, 3792; d) J. Hernandez-Trujillo, R. F. W. Bader, *J. Phys. Chem. A* **2000**, 104, 1779.
- [18] a) P. Coppens, *X-Ray Charge Densities and Chemical Bonding*, Oxford University Press, Oxford, **1997**; b) *Electron Distributions and Chemical Bonds* (Eds.: P. Coppens, M. B. Hall), Plenum Press, New York, **1982**; c) J. D. Dunitz, *X-ray Analysis and the Structure of Organic Molecules*, Cornell University Press, Ithaca, New York, **1979**, Chapter 8.
- [19] For some leading references on ELF, see: a) A. D. Becke, K. E. Edgecombe, *J. Chem. Phys.* **1990**, 92, 5379; b) A. Savin, O. Jepsen, J. Flad, O. K. Anderson, H. Preuss, H. G. von Schnering, *Angew. Chem.* **1992**, 104, 186; *Angew. Chem. Int. Ed. Engl.* **1992**, 31, 187; c) B. Silvi, A. Savin, *Nature* **1994**, 371, 683; d) A. Savin, R. Nesper, S. Wengert, T. F. Fässler, *Angew. Chem.* **1997**, 109, 1892; *Angew. Chem. Int. Ed. Engl.* **1997**, 36, 1809; e) B. Silvi, *J. Phys. Chem. A* **2003**, 107, 3081.
- [20] R. Luser, A. Beltrán, J. Andrés, S. Noury, B. Silvi, *J. Comput. Chem.* **1999**, 20, 1517.
- [21] See however, discussions of the covalency of F_2 and other molecules, in: a) D. Cremer, E. Kraka, *Angew. Chem.* **1984**, 96, 612; *Angew. Chem. Int. Ed. Engl.* **1984**, 23, 627; b) A. A. Low, M. B. Hall in *Theoretical Models of Chemical Bonding*, Part 2 (Ed.: Z. B. Maksic), Springer, New York, **1990**, pp. 544–591; c) E. Kraka, D. Cremer in *Theoretical Models of Chemical Bonding*, Part 2 (Ed.: Z. B. Maksic), Springer, New York, pp. 457–543; d) W. H. E. Schwarz, P. Valtazanos, K. Ruedenberg, *Theor. Chim. Acta* **1985**, 68, 471; e) L. Rincon, R. Almeida, *J. Phys. Chem. A* **1998**, 102, 9244–9254.
- [22] For a recent summary of VB methods, see: *Valence Bond Theory* (Ed.: D. L. Cooper), Elsevier, Amsterdam, **2002**.
- [23] For the leading BOVB references, see: a) P. C. Hiberty, J. P. Flament, E. Noizet, *Chem. Phys. Lett.* **1992**, 189, 259; b) P. C. Hiberty in *Modern Electronic Structure Theory and Applications in Organic Chemistry* (Ed.: E. R. Davidson), World Scientific, River Edge, New York, **1997**, pp. 289–367; c) P. C. Hiberty, S. Shaik, *Theor. Chem. Acc.* **2002**, 108, 255.
- [24] For leading VBCI references, see: a) W. Wu, L. Song, Z. Cao, Q. Zhang, S. Shaik, *J. Phys. Chem. A* **2002**, 106, 2721; b) L. Song, W. Wu, Q. Zhang, S. Shaik, *J. Comput. Chem.* **2004**, 25, 472–478.
- [25] For VBSCF, see: a) J. Verbeek, J. H. van Lenthe, *J. Mol. Struct.* **1991**, 229, 115; b) J. H. van Lenthe, F. Dijkstra, W. A. Havenith in *Valence Bond Theory* (Ed.: D. L. Cooper), Elsevier, Amsterdam, **2002**, pp. 79–116.
- [26] H. B. Chirgwin, C. A. Coulson, *Proc. Roy. Soc. A. (London)* **1950**, 2, 196.
- [27] W. Wu, L. Song, Y. Mo, Q. Zhang, *XIAMEN-99 - An Ab Initio Spin-free Valence Bond Program*, Xiamen University, Xiamen, **1999**.
- [28] M. J. Frisch, G. W. Trucks, H. B. Schlegel, G. E. Scuseria, M. A. Robb, J. R. Cheeseman, V. G. Zakrzewski, J. A. Montgomery, Jr., R. E. Stratmann, J. C. Burant, S. Dapprich, J. M. Millam, A. D. Daniels, K. N. Kudin, M. C. Strain, O. Farkas, J. Tomasi, V. Barone, M. Cossi, R. Cammi, B. Mennucci, C. Pomelli, C. Adamo, S. Clifford, J. Ochterski, G. A. Petersson, P. Y. Ayala, Q. Cui, K. Morokuma, D. K. Malick, A. D. Rabuck, K. Raghavachari, J. B. Foresman, J. Cioslowski, J. V. Ortiz, A. G. Baboul, B. B. Stefanov, G. Liu, A. Liashenko, P. Piskorz, I. Komaromi, R. Gomperts, R. L. Martin, D. J. Fox, T.

- Keith, M. A. Al-Laham, C. Y. Peng, A. Nanayakkara, M. Challacombe, P. M. W. Gill, B. Johnson, W. Chen, M. W. Wong, J. L. Andres, C. Gonzalez, M. Head-Gordon, E. Replogle, J. A. Pople, *GAUSSIAN 98*, Gaussian, Inc., Pittsburgh, PA, **1998**.
- [29] D. E. Woon, T. H. Dunning Jr., *J. Chem. Phys.* **1993**, *98*, 1358.
- [30] J. A. Pople, M. Head-Gordon, K. Raghavachari, *J. Chem. Phys.* **1987**, *87*, 5968.
- [31] a) S. Noury, X. Krokidis, F. Fuster, B. Silvi, *TopMod Package*, **1997**; b) S. Noury, X. Krokidis, F. Fuster, B. Silvi, *Comput. In Chem.* **1999**, *23*, 597.
- [32] A. D. Becke, *J. Chem. Phys.* **1993**, *98*, 5648–5652; A. D. Becke, *Phys. Rev. A* **1988**, *38*, 3098–3100; C. Lee, Y. Yang, R. G. Parr, *Phys. Rev. B* **1988**, *37*, 785; B. Miechlich, A. Savin, H. Stoll, H. Preuss, *Chem. Phys. Lett.* **1989**, *157*, 200.
- [33] It can be shown that the formally covalent GVB wave function of F–F involves in fact a mixture of the classical and covalent and ionic structures of the bond (See: P. C. Hiberty, D. L. Cooper, *J. Mol. Struct.* **1988**, *169*, 437). The bond energy of this wave function is rather poor, $15.7 \text{ kcal mol}^{-1}$,^[23] and only further extensive CI, or explicit treatment of the ionic structures as in the BOVB method lead to the correct bond energy, about 36 kcal mol^{-1} . Thus bonding in F–F originates from the response of the electronic structure to the fluctuation of the electron pair density from the average density.
- [34] For “dynamic ionicity”, see: D. Maynau, J.-P. Malrieu, *J. Chim. Phys.* **1988**, *88*, 3163.
- [35] R. T. Sanderson, *Polar Covalence*, Academic Press, New York, **1983**.
- [36] The electronegativity and orbital compactness are proportional to the effective nuclear charge of the atom. See, for example: a) A. L. Allerd, E. Rochow, *J. Inorg. Nucl. Chem.* **1958**, *5*, 264; b) Ref. 35, pp. 15–21.
- [37] For analyses of electronegativity and the sum quantity, see: L. C. Allen, *Electronegativity and the Periodic Table in Encyclopedia of Computational Chemistry*, Vol. 2 (Eds.: P. von R. Schleyer, N. L. Allinger, T. Clark, J. Gasteiger, P. A. Kollman, H. F. Schaefer III, P. R. Schreiner), Wiley, Chichester, UK, **1998**, pp. 835–852.
- [38] For the role of kinetic and potential energy components in bonding, see, for example: a) K. Ruedenberg, *Rev. Mod. Phys.* **1962**, *34*, 326; b) R. F. W. Bader, H. J. T. Preston, *Int. J. Quant. Chem.* **1969**, *3*, 327; c) W. H. E. Schwarz, T. Bitter, *Ber. Bunsenges. Phys. Chem.* **1976**, *80*, 1231; d) W. Kutzelnigg in *Theoretical Models of Chemical Bonding*, Part. 2 (Ed.: Z. B. Maksic), Springer, New York, **1990**, pp. 1–44; e) M. J. Feinberg, K. Ruedenberg, *J. Chem. Phys.* **1971**, *54*, 1495; f) C. Q. Wilson, W. A. Goddard III, *Theor. Chim. Acta* **1972**, *26*, 195; g) A. Rozendaal, E. J. Baerends, *Chem. Phys.* **1985**, *95*, 57–91.
- [39] P. C. Hiberty, L-BOVB/6–31G** calculations, unpublished data.
- [40] For a valence orbital in a central field, the potential energy varies in proportion to ζ (the orbital exponent), while the kinetic energy changes as ζ^2 .
- [41] a) H. Z. Hellman, *Physik* **1933**, *85*, 180; *Einführung in die Quantenchemie*, Leipzig, **1937**, pp. 285; b) R. P. Feynman, *Phys. Rev.* **1939**, *56*, 340.
- [42] a) T. Berlin, *J. Chem. Phys.* **1951**, *19*, 208; b) see, however, H. Silberbach, *J. Chem. Phys.* **1991**, *94*, 2977–2985.
- [43] See, for example: a) J. D. Dunitz, P. Seiler, *J. Am. Chem. Soc.* **1983**, *105*, 7056; b) J. D. Dunitz, W. B. Schweizer, P. Seiler, *Helv. Chim. Acta* **1983**, *66*, 123; c) J.-M. Savariault, M. S. Lehmann, *J. Am. Chem. Soc.* **1980**, *102*, 1298; d) P. Coppens, M. S. Lehmann, *Acta Crystallogr. Sect. B* **1977**, *32*, 1777; e) P. Coppens, Y. W. Yang, R. H. Blessing, W. F. Cooper, F. K. Larsen, *J. Am. Chem. Soc.* **1977**, *99*, 760; f) Y. W. Yang, P. Coppens, *Solid State Commun.* **1974**, *15*, 1555.
- [44] J. J. Engelberts, *PhD Thesis*, University of Utrecht, **2005**.
- [45] S. Shaik, A. Shurki, *Angew. Chem.* **1999**, *111*, 616; *Angew. Chem. Int. Ed.* **1999**, *38*, 586.
- [46] P. C. Hiberty, L. Song, W. Wu., S. Shaik, unpublished results.
- [47] a) S. V. O’Neal, H. F. Schaefer III, C. F. Bender, *Proc. Natl. Acad. Sci. USA* **1974**, *71*, 104; b) T. H. Dunning Jr., *J. Phys. Chem.* **1984**, *88*, 2469; c) C. F. Bender, B. J. Garrison, H. F. Schaefer III, *J. Chem. Phys.* **1975**, *62*, 1188; d) A. F. Voter, W. A. Goddard III, *J. Chem. Phys.* **1981**, *75*, 3638; e) K. D. Dobbs, C. A. Dixon, *J. Phys. Chem.* **1993**, *97*, 2085.
- [48] F. E. Bartoszek, D. M. Mano, J. C. Polanyi, *J. Chem. Phys.* **1978**, *69*, 933.
- [49] In VB theory, the repulsive interactions arise from identical spins of electrons in two overlapping orbitals. See: a) S. Shaik in *New Theoretical Concepts for Understanding Organic Reactions* (Eds.: J. Bertran, I. G. Csizmadia), NATO ASI Series, C267, Kluwer Academic Publ, **1989**, pp. 165–217; b) J. P. Malrieu, D. Maynau, *J. Am. Chem. Soc.* **1984**, *106*, 3021; c) S. Shaik, P. C. Hiberty, *Rev. Comput. Chem.* **2004**, *20*, 1.
- [50] L. Maron, L. Perrin, O. Eisenstein, *Dalton Trans.* **2003**, 4313.
- [51] A. A. Fiorillo, J. M. Galbraith, *J. Phys. Chem. A* **2004**, *108*, 5126.
- [52] M. L. Coote, A. Pross, L. Radom, *Org. Lett.* **2003**, *5*, 4689.
- [53] J. M. Galbraith, A. Shurki, S. Shaik, *J. Phys. Chem.* **2000**, *104*, 1262.
- [54] a) See, for example, the RE_{CS} for $(FHF)^-$ in Reference [45] above. The bonding in XeF_2 is CS bonding since it arises solely from the mixing of the ionic structures, $F^- + Xe-F$ and $F-Xe^+ F^-$ into the no-bond structure $F^+ Xe^- F$. See: S. S. Shaik, *Valence Bond Mixing: The LEGO Way. From Resonating Bonds to Resonating Transition States*, in *An Encomium to Linus Pauling. Molecules in Natural Science and Medicine*, (Eds.: Z. B. Maksic, M. E. Maksic), Ellis Horwood, London, **1991**.

Received: March 9, 2005
Published online: August 5, 2005